Bioactive Materials 2 (2017) 10–18

Contents lists available at ScienceDirect

Bioactive Materials

journal homepage: http://www.keaipublishing.com/en/journals/bioactive-materials/

In vitro degradation and surface bioactivity of iron-matrix composites containing silicate-based bioceramic

Sanguo Wang [a, b, 1], Yachen Xu [c, 1], Jie Zhou [d], Haiyan Li [c], Jiang Chang [a], Zhiguang Huan [a, *]

[a] Shanghai Institute of Ceramics, Chinese Academy of Sciences, 1295 Dingxi Road, Shanghai 200050, China
[b] School of Materials Science and Engineering, Shanghai Institute of Technology, 120 Caobao Road, Shanghai 200235, China
[c] Med-X Research Institute, School of Biomedical Engineering, Shanghai Jiao Tong University, 1954 Huashan Road, Shanghai 200030, China
[d] Department of Biomechanical Engineering, Delft University of Technology, Mekelweg 2, 2628 CD Delft, The Netherlands

ARTICLE INFO

Article history:
Received 23 July 2016
Received in revised form
30 November 2016
Accepted 1 December 2016
Available online 20 December 2016

Keywords:
Iron
Calcium silicate
Composite
Biodegradation
Bioactivity
Implant

ABSTRACT

Iron-matrix composites with calcium silicate (CS) bioceramic as the reinforcing phase were fabricated through powder metallurgy processes. The microstructures, mechanical properties, apatite deposition and biodegradation behavior of the Fe-CS composites, as well as cell attachment and proliferation on their surfaces, were characterized. In the range of CS weight percentages selected in this study, the composites possessed compact structures and showed differently decreased bending strengths as compared with pure iron. Immersion tests in simulated body fluid (SBF) revealed substantially enhanced deposition of CaP on the surfaces of the composites as well as enhanced degradation rates as compared with pure iron. In addition, the composite containing 20% CS showed a superior ability to stimulate hBMSCs proliferation when compared to pure iron. Our results suggest that incorporating calcium silicate particles into iron could be an effective approach to developing iron-based biodegradable bone implants with improved biomedical performance.

1. Introduction

Over the last decade, biodegradable metallic implants for orthopedic applications have gained substantial interest, as they can avoid the negative effects related to the use of permanent implants, such as inflammation and stress shielding [1,2]. In recent years, iron and its alloys have been proposed as candidate materials potentially for orthopedic applications, especially for the applications where strong mechanical support during the bone healing process is needed [3]. Although concerns over the potential toxic effect due to the excessive intake of the iron element have been raised [4], a number of in vitro and in vivo studies on iron-based implants have demonstrated good biocompatibility and biosafety of pure iron for orthopedic applications [5–7]. However, being similar to Mg-based biodegradable materials, iron-based materials developed so far have shown a number of deficiencies in biomedical performance. One of the deficiencies, probably being the biggest one, concerns the rather low degradation rate of iron. An in vivo study conducted by Kraus et al. [8], for example, showed that the degradation rate of the iron implant over an implantation period of 52 weeks was inadequately low and thus its suitability as a temporary implant for osteo-synthesis applications became doubtful. In addition, the surface bioactivity of iron would need to be improved, as it was demonstrated by other researchers that the virtual inability of iron to stimulate bone formation was quite similar to that of bio-inert stainless steel [9].

It is obvious that further research efforts are needed to accelerate the degradation of iron-based biomaterials and in the meantime to enhance their bioactivity. To date, most of the research on the subject has been focused on accelerating the degradation of iron-based biomaterials by means of alloying. It has been found that alloying iron with elements such as manganese, palladium or silver can indeed enhance its degradation rate [5,10,11]. However, in order to achieve effective increases in degradation rate, these alloying elements have to be added in very large weight percentages, e.g., greater than 15% Mn [11], which may lead to uncertainties about the biocompatibility of the alloys. Moreover, alloying with these elements is unlikely to improve the

* Corresponding author.
E-mail address: huanzhiguang@mail.sic.ac.cn (Z. Huan).
Peer review under responsibility of KeAi Communications Co., Ltd.
[1] These two authors contributed equally to the work.

http://dx.doi.org/10.1016/j.bioactmat.2016.12.001

bioactivity of iron.

In recent years, the development of metal matrix composites (MMCs) has been recognized as an alternative approach to developing iron-based biomaterials with accelerated degradation rates. Ulum et al. [12], for example, developed a series of biocomposites by incorporating hydroxyapatite (HA), β-tricalcium phosphate (TCP) or HA-TCP mixtures into pure iron. The degradation rates of the biocomposites were found to be slightly higher than the degradation of pure iron, which was attributed to the presence of these bioceramics in the composite structure. From the results of an in vivo evaluation in their follow-up study, Ulum et al. [9] confirmed the enhanced bioactivity of the composites as compared with pure iron.

Although the research in this field has yet been quite scarce, the feasibility of improving the degradation rate and bioactivity of iron by incorporating bioceramic particles has been well acknowledged. Nevertheless, more research efforts are needed to optimize the compositions of iron-matrix composites in order to achieve more effective improvements in degradation and bioactivity properties. For example, one may hypothesize that the use of bioceramic having a higher degradation rate and bioactivity than HA and TCP can lead to the attainment of the desired improvements. Another possible approach is to enlarge the weight percentages or volume fractions of bioceramic particles added to the iron matrix.

The aim of the present study was to develop a new class of iron-matrix composites by optimizing both the selection and the content of the bioceramic phase. In this study, instead of calcium phosphate-based bioceramics such as HA and TCP, the calcium silicate (CS) bioceramic was chosen as the reinforcement phase for the iron matrix. Among all the silicate-based bioceramics, calcium silicate (CS) presents the simplest chemical composition. A number of studies have already confirmed its superior biodegradability and bioactivity, as compared with calcium phosphate-based bioceramics, including HA and TCP [13–15]. These characteristic properties make CS an interesting reinforcement material for pure iron, when enhanced biomedical properties are desired. In addition, in comparison with the relatively low weight percentages (around 10%) of bioceramics in the biocomposites found in the literature [9,12,16], in this study, the weight percentage of CS incorporated into the iron matrix was significantly increased in order to clarify the effect of CS addition on the degradation behavior and surface bioactivity of the biocomposites. With the Fe-CS biocomposites successfully prepared, their microstructures, mechanical performance and degradation behavior were characterized. Furthermore, the in vitro surface bioactivity of the composite materials was evaluated by means of immersion tests in simulated body fluid (SBF) and their in vitro cytotoxicity was evaluated through direct contact with human bone marrow stromal cells (hBMSCs).

2. Materials and methods

2.1. Composite fabrication and structural characterization

An iron powder with 99.5% purity and a mean particle size of 20 μm (Haotian Nano Technology, China) and a CS powder were used as the starting materials. The CS ($CaSiO_3$) powder was synthesized by means of a chemical precipitation method using $Ca(NO_3)\cdot 4H_2O$ and $Na_2SiO_3\cdot 9H_2O$ as the raw materials according to our previous study [17] and it had a mean powder particle size of 10 μm. The fabrication of pure iron and Fe-CS composites was based on a powder metallurgy method. Firstly, the iron and CS powders were mixed for 1 h to prepare mixtures with 0, 20, 30 and 40% CS by weight, and the materials were denoted as Fe, Fe-20CS, Fe-30CS and Fe-40CS, respectively. Prior to sintering, the mixtures were uniaxially pressed under a pressure of 8 MPa into pellets with a diameter of 10 mm. The pellets were heated at a rate of 5 °C/min to 1120 °C in a tube furnace with an argon atmosphere and then sintered for 2 h, followed by furnace cooling to room temperature.

For microstructural characterization, the as-fabricated iron and Fe-CS composite samples were ground by sandpapers down to a grid size of 2400 and polished with a lubricant containing 3 μm diamond particles. An X-ray diffractometer (XRD; Geiger-Flex, Rigaku, Japan) was used to identify the phases in the composite materials, for which the 2-theta angles were set from 10 to 80°. The surface morphologies and elemental compositions of the Fe-CS composites were investigated by using a scanning electron microscope (SEM; JSM-6700F, JEOL, Japan) equipped with an energy dispersive X-ray (EDX) spectrometer (INCA Energy, Oxford Instruments).

To confirm the structure compactness of metallographic samples, the as-sintered density values of specimens were determined by using a densimeter (ET-320VP, Etanln, China). For reproducibility, three specimens were used.

2.2. Mechanical tests

The mechanical properties of the materials were evaluated in terms of compressive and bending strengths. To determine the compressive strengths of the materials, cylindrical specimens with a diameter of 10 mm and a height of 15 mm were prepared. Compression tests were carried out at room temperature using a universal testing machine (Instron 5566 with a force capacity of 10 kN, USA), according to the ASTM E9-09 standard [18]. To determine the bending strengths, specimens with dimensions of $4 \times 4 \times 50$ mm^3 were prepared. Three-point bending tests with a span of 45 mm between the two supporting pins were carried out at a crosshead speed of 1 mm/min (Instron-5566, USA). At least six repeat specimens were used in the compression and bending tests.

2.3. Static immersion tests in simulated body fluid

To evaluate the mineralization ability of the Fe-CS composites, disk-shaped specimens with a diameter of 10 mm and a height of 2 mm were prepared. Simulated body fluid (SBF) was prepared according to the method described by Kokubo [19] and its composition is given in Table 1. Specimens were soaked in SBF and placed a shaking water bath at a constant temperature of 37 °C. The ratio of the surface area of the specimen to the volume of SBF was set to 0.1 cm^2/ml [19]. The immersion medium was completely refreshed once a day. After 7 days of immersion, the specimens were taken out of the immersion medium, rinsed with deionized water and then air-dried. The morphologies and elemental compositions of the deposited layer on the surfaces of the specimens were characterized by using SEM (Hitachi S8220, Japan) equipped with EDX.

The in vitro degradation behavior of the Fe-CS composites was evaluated by performing weight loss measurement over a total period of 1 month. Disk-shaped specimens with a diameter of

Table 1
Composition of SBF (1000 mL) used in the immersion tests.

	NaCl	$NaHCO_3$	KCl	$K_2HPO_4\cdot 3H_2O$	$MgCl_2\cdot 6H_2O$
Amount	8.035 g	0.355 g	0.255 g	0.231 g	0.311 g
Purity (%)	99.5	99.5	99.5	99.0	98.0
	1.0M-HCl	**$CaCl_2$**	**Na_2SO_4**	**Tris**	**1.0M-HCl**
Amount	39 mL	0.292 g	0.072 g	6.118 g	0–5 mL
Purity (%)	–	95.0	99.0	99.0	–

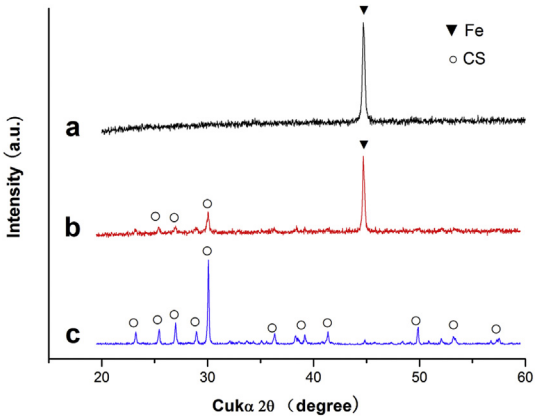

Fig. 1. XRD spectra of pure Fe (a), Fe-20CS composite (b) and CS (c).

10 mm and a thickness of 2 mm were ground, polished and weighed before testing. The specimens were then soaked in SBF. The immersion tests were performed at 37.0 °C in a water bath at a constant shaking speed of 120 rpm. For each specimen, a 50 mL Tris-HCl buffer solution was used, considering that the volume/surface area (SV/SA) ratio would not cause any significant influence on the corrosion rate of the specimen when it was higher than 6.7 [20]. The immersion medium was refreshed once a week. After a pre-selected period, specimens were taken out of the soaking medium, rinsed by distilled water and ethanol, and dried by flowing hot air. The corrosion products were removed by using a solution composed of 100 mL HCl, 5 g $SnCl_2$ and 2 g Sb_2O_3 [21,22]. The specimens were then dried in the same way as after specimen collection. Subsequently, the specimens were weighed and the corrosion rate (CR) was calculated according to Eq. (1):

$$CR = \Delta m/At \quad (1)$$

where CR is the corrosion rate (g m^{-2} d^{-1}), Δm the weight loss of the specimen (g), A the original specimen surface area exposed to the soaking medium (m^2), and t the immersion time (d). For reproducibility, three specimens were used for each group.

2.4. Cytocompatibility tests

2.4.1. Cell isolation and culture

Human bone mesenchymal stem cells (hBMSCs) were isolated from human bone marrow according to the method reported previously [23]. The procedure was approved by the Ethics Committee of Shanghai Jiao Tong University. Total bone mesenchymal stem cell culture medium (Cyagen Biosciences, USA), consisting of bone mesenchymal stem cell basal medium, 5% fetal bovine serum, 1% stem cell growth supplement and 1% penicillin/streptomycin, was used as hBMSCs' culture medium. The cell culture medium was replaced every 2 days. Only early passages (i.e., passages 2–7) of the hBMSCs were used in this study.

2.4.2. Immunofluorescence staining

To investigate cell morphology, adhesion and distribution on iron and Fe-CS composite plates, F-actin staining was applied on hBMSCs after hBMSCs had been cultured for 24 h. Rhodamine phalloidin R415 (Invitrogen, USA) and 4-6-diamidino-2-phenylindole (DAPI) (FluoProbes, USA) were applied to stain actin filaments and the nuclei of hBMSCs, according to the supplier's procedure. The cytoskeletal and nuclear organizations were observed and photographed using a confocal microscope (Leica TCS SP5, Germany) equipped with a CCD camera (Leica DFC 420C, Germany).

2.4.3. hBMSCs proliferation assay

To quantify the proliferation of cells on iron and Fe-CS composite plates, hBMSCs were seeded on Fe, Fe-20CS and Fe-40CS in 48-well plates at a density of 5×10^3 cells per well and cultured in a humidified 37°C/5% CO_2 incubator with the total bone mesenchymal stem cell culture medium for 1, 3 and 7 days. Cells cultured on iron plates were regarded as controls. The medium was replaced

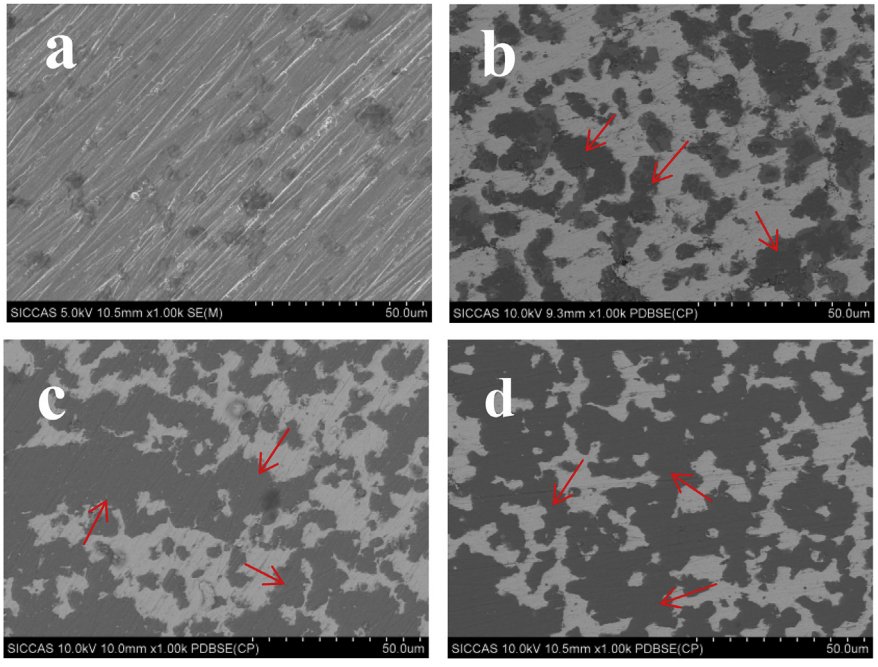

Fig. 2. SEM micrographs of the as-fabricated pure Fe (a), Fe-20CS (b), Fe-30CS (c) and Fe-40CS (d) composites. Red arrows point to the CS phase in the composites.

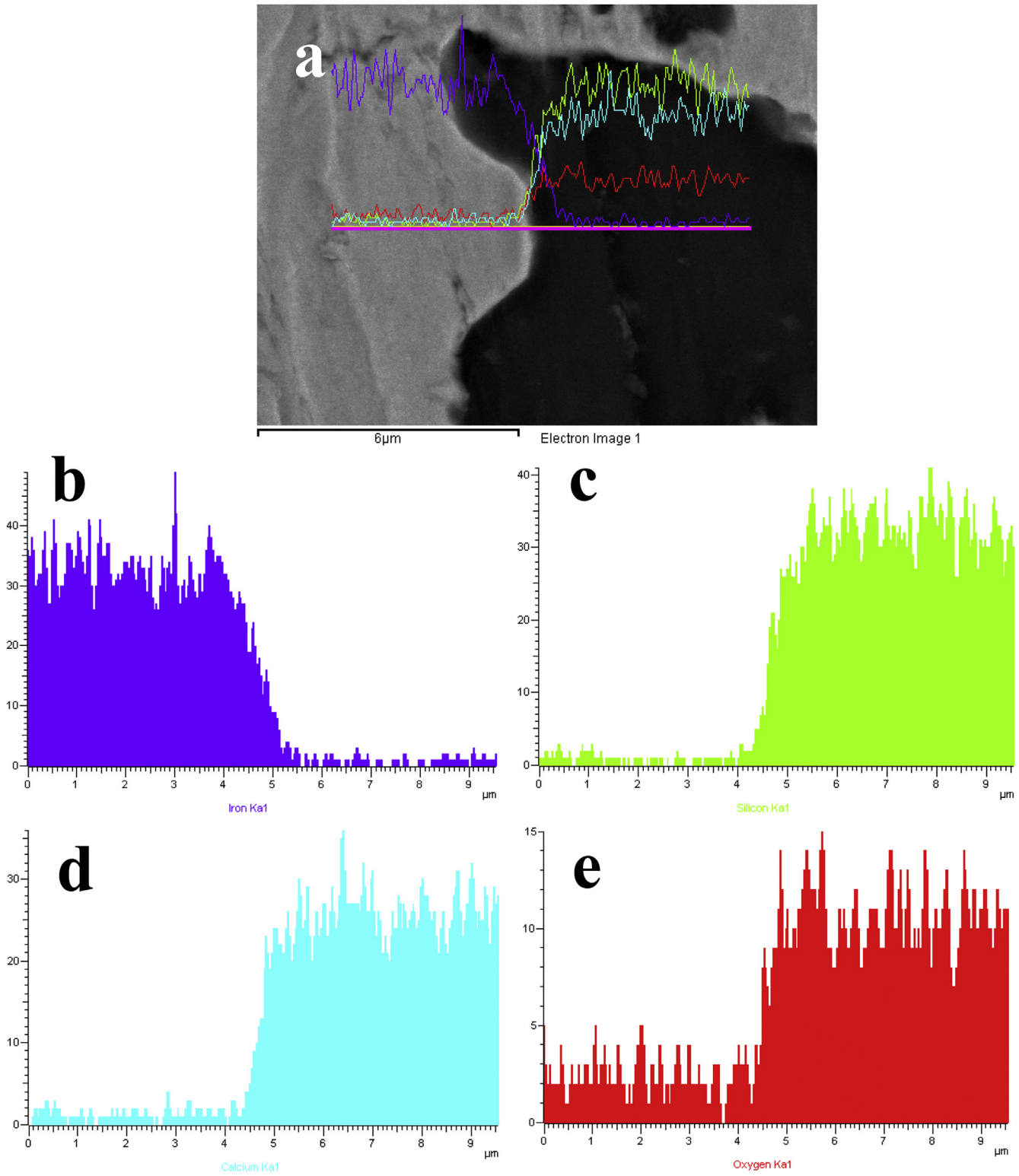

Fig. 3. SEM morphology of the Fe-30CS composite (a), on which a line scan EDX analysis across a boundary region from the Fe matrix to a CS particle was performed to reveal the elemental distributions of Fe (b), Si (c), Ca (d) and O (e).

every 2 days. At each selected time point, a Cell Counting Kit (CCK)-8 assay (Beyotime, China) was performed according to the manufacturer's instructions to evaluate cell proliferation. The absorbance of the supernatant was measured by an enzyme-linked immunoadsorbent assay microplate reader (Synergy 2, Bio-TEK) at a wavelength of 450 nm (n = 6).

2.4.4. Statistical analysis

The results were expressed as mean ± standard deviation. Three independent experiments were carried out and at least six samples

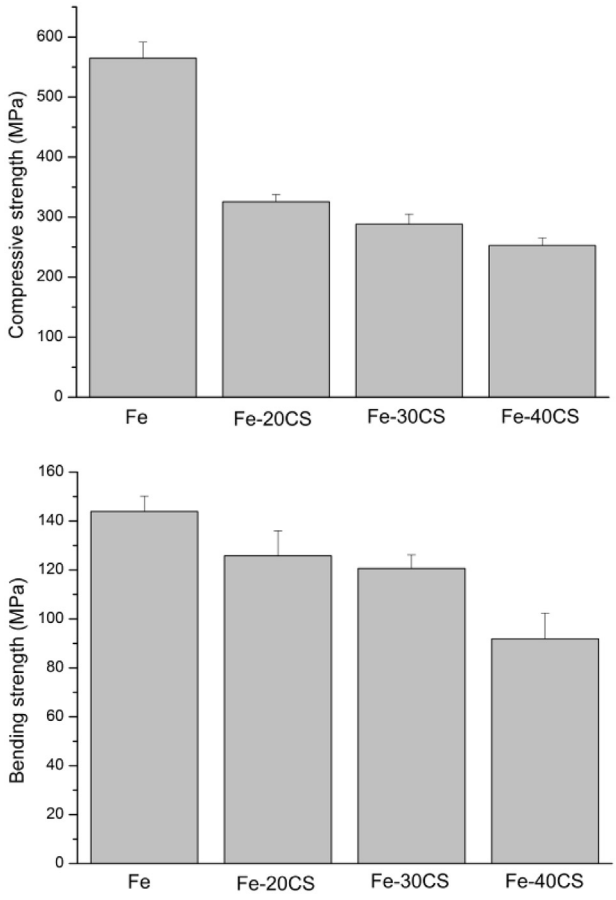

Fig. 4. Compressive strengths (a) and bending strengths (b) of the Fe-CS composites with different weight percentages of CS.

per each test were taken for statistical analysis. Statistical significance between two groups was calculated using two-way analysis of variance (ANOVA) and performed with a Student's *t*-test program. Differences were considered significant when $p < 0.05$ (*) or $p < 0.01$ (**).

3. Results and discussion

3.1. Phasic and microstructural characteristics of the Fe-CS composites

Fig. 1 shows the XRD patterns of pure iron, Fe-20%CS and pure CS. Only the peaks of the Fe phase and CS phase were identified in the XRD patterns of pure Fe and CS samples, respectively. For the Fe-20%CS composite, the peaks corresponding to Fe and CS were identified. No new crystalline compounds, such as Fe_3O_4 or intermetallic compounds, could be detected. The results of the XRD analysis indicated that there were no severe chemical interactions occurring between Fe and CS during the mixing, compaction and sintering processes, suggesting that Fe and CS in the composites could maintain their individual chemical properties after composite fabrication.

The microstructural features of pure iron and the Fe-CS composites, as observed using the back-scattered electron mode in SEM, are presented in Fig. 2. It can be seen in Fig. 2a that the pure iron sample had a compact microstructure and a relative sintered density larger than 99%, but the morphological characteristics of a few original powder particles were still discernible. This observation was in agreement with the findings in earlier studies on the sintering behavior of powdered iron alloy under similar conditions [24]. By contrast, the microstructures of the Fe-CS composites consisted of two distinct phases, i.e., a grey background and homogeneously distributed black particles. It was obvious that the grey background and black particles belonged to the Fe and CS phases, respectively. All the Fe-CS composites containing up to 40% CS exhibited compact structures and the homogeneously distributed CS particle all over the Fe matrix. It could be expected that these Fe-CS composites would possess homogeneous bulk properties. It was however noted that as the content of CS became higher than 30%, CS particles became in contact with each other and tended to merge to form larger CS clusters in the structure (Fig. 2c–d). As the sintering temperature of the composites used in the present study was slightly higher than the typical sintering temperature of pure CS powder (around 1100 °C) [25], it was reasonable to assume that the sintering of CS took place together with that of iron particles and Fe-CS particles, given that a larger CS content increased the chance for CS particles to be neighboring ones. Clearly, the sintering taking place between CS particles would benefit the formation of the compact structures of the Fe-CS composites.

From a composite material design point of view, it is of great importance to ensure strong bonding at the interfaces between the metal matrix and ceramic particles, as it is well known that the interfaces often act as the preferential sites for the initiation of cracks and are responsible for the occurrence of premature failure once the stress on the composite exceeds a limit [26,27]. In this study, the interfaces between the Fe phase and CS phase in the Fe-CS composites were investigated by means of EDX line scan analysis. The results obtained from the analysis of the Fe-30%CS composite served as a representative and are presented in Fig. 3. It is clear that the sintering process in this study yielded sound Fe—CS interfaces that were free from any discernible pores. In addition, it was found that there was slight elemental diffusion from the Fe matrix towards CS particles (Fig. 3a–b) and the depth of penetration was about several tens of nanometers. As the XRD analysis of the composites (Fig. 1) did not reveal the formation of any compounds formed between the Fe and CS phases, iron must have diffused and been incorporate into the crystal lattice of CS near the interfaces. Similar results have been reported in another study on Fe-incorporated hydroxyapatite (HA) bioceramics [28]. The atomic diffusion from the Fe matrix towards CS particles may be favorable for the formation of a strengthened bonding between the two phases, which is desirable because premature failure due to weak interface bonding is often a serious problem for MMCs [26].

3.2. Mechanical properties of the Fe-CS composites

The compressive and bending strengths of the Fe-CS composites as compared with those of pure iron are presented in Fig. 4a and Fig. 4b, respectively. The compressive strengths of the Fe-CS composites were determined from the compression curves at a strain of 30%. It can be seen that the compressive strengths of the Fe-CS composites were all significantly lower than the strength of pure iron and the compressive strength decreased with increasing content of CS particles in the composite. The lowered compressive strengths could be attributed to the inherent brittle nature of the CS ceramic, as well as its large amounts in the composites [29]. It is however of great interest to note that, being different from the compressive strengths, the bending strengths of the composites were not so much decreased from the bending strength of pure iron, when the weight percentage did not exceed 30% (Fig. 4b). We believed that such a phenomenon was due to strong interface bonding between the Fe matrix and CS particles, as indicated by the

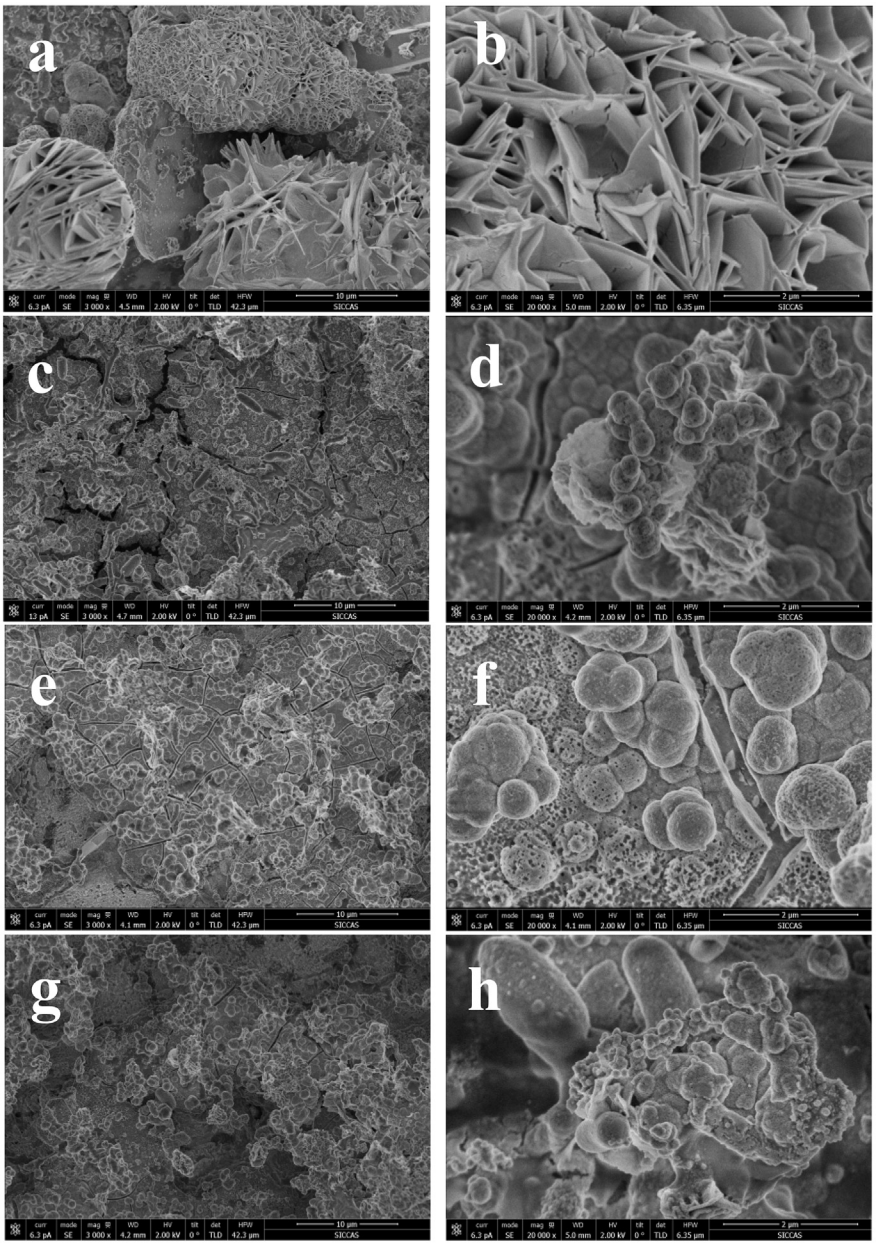

Fig. 5. SEM morphologies of pure Fe (a, b), Fe-20CS (c, d), Fe-30CS (e, f) and Fe-40CS (g, h) composites after immersion in SBF for 7 days. Images b, d, f and h present the surface morphology of the corrosion layer at higher magnifications.

Table 2
Results of the EDS elemental analysis on the surfaces of pure-Fe and Fe-CS composite samples after immersion in SBF for 7 days.

	Fe (at.%)	Ca (at.%)	Si (at.%)	P (at.%)	O (at.%)
Pure Fe	19.83	0.50	/	15.79	61.84
Fe-20CS	17.85	5.00	0.70	14.03	59.90
Fe-30CS	13.65	7.05	0.22	12.92	56.59
Fe-40CS	12.47	7.37	2.70	11.96	58.80

interface analysis shown in Fig. 3 [30]. However, an excessive addition of CS particles to iron, namely 40% in the current study, indeed caused a significant decrease in the bending strength of the composite, which must have been related to the relatively low bending strength of the CS ceramic [31]. Further investigation is needed to reveal the underlying mechanisms of early crack initiation and propagation, leading to the reduced mechanical properties of the Fe-CS composites, especially when the addition of CS exceeds 20%.

The compressive strength of human compact bone ranges from 130 to 240 MPa [32] and its bending strength ranges from 103.5 to 225.0 MPa [33]. In the present study, the compressive and bending strengths of the iron-matrix composites containing 20% and 30% CS were higher than the high-end value of compressive strength and the low-end value of bending strength of human compact bone, respectively, suggesting their suitability for the repair of bone defects in load-bearing sites. However, as the content of CS increased to 40%, the bending strength of the composite was lower than the low end value of human compact bone, which would mean that this composite might not be able to provide sufficient mechanical support to resist flexural loading after implantation.

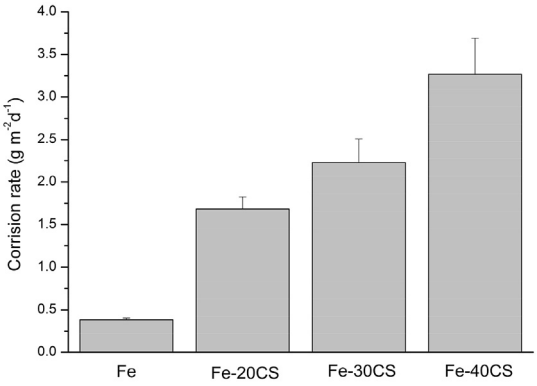

Fig. 6. Degradation rates determined from the mass loss measurements of pure Fe and the Fe-CS composites with different weight percentages of CS.

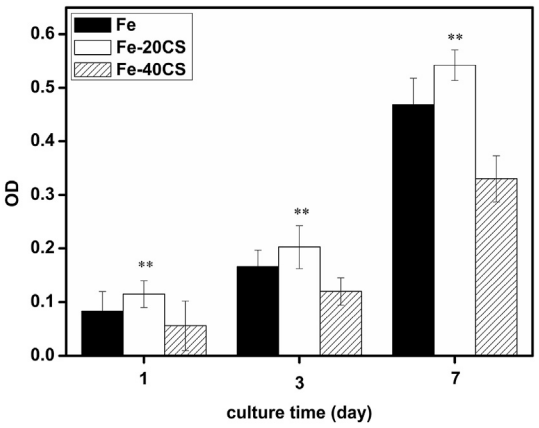

Fig. 8. Proliferation of hBMSCs cultured on the surfaces of Fe, Fe-20CS and Fe-40CS composites. ** represents $P < 0.01$ when the data are compared with the control (pure Fe).

3.3. *Apatite formation ability and biodegradation rates of the Fe-CS composites*

After immersion in the SBF solution for 7 days, both pure Fe and Fe-CS MMCs specimens were covered by a corrosion layer. The corrosion layer on pure iron had a dark brown color, while that on the composites had a light brown color. The SEM images of the corrosion layer on the surfaces of pure iron and the Fe-CS composites are shown in Fig. 5. It can be seen that the corrosion layer on the surface of pure iron after immersion in SBF for 7 days was composed of plate-like crystals (Fig. 5a). By contrast, the corrosion layer on the surfaces of the Fe-CS composites was composed of agglomerates of lath-like tiny crystals, regardless of the content of CS in the composites. The elemental compositions of the corrosion product formed on Fe and the Fe-CS composites are presented in Table 2. The corrosion product on pure iron after immersion in SBF for 7 days was rich in Fe, O and P, and only a small amount of Ca was detected. The corrosion layer was considered to be mainly composed of hydrated iron oxide and iron phosphate, being similar to those reported in previous studies [21,22,24]. On the surfaces of the composites also after immersion in SBF for 7 days, however, a larger amount of Ca was detected and the Ca concentration increased with increasing CS content in the composite. Clearly, the presence of CS indeed encouraged the deposition of calcium phosphate, which was attributed to the excellent ability of CS to induce the formation of a CaP layer as a result of interactions with SBF [14,15]. The role of the CaP layer in affecting the progress of corrosion will be ascertained in further research.

The degradation rates of the Fe-CS composites as compared with the degradation rate of pure iron during the immersion tests in SBF are shown in Fig. 6. Both pure Fe and Fe-CS MMCs specimens maintained their structural integrity over the whole period of the immersion tests for one month. It can be seen that the degradation rates of the Fe-CS composites were significantly higher than the degradation rate of pure iron and the rate was enhanced with increasing content of CS particles in the composite. Such a trend could be explained by the relatively higher solubility of CS in the physiological environment [14] through decomposition of $CaSiO_3$ and then interaction with water. The degradation rate of the Fe-40CS composite, being the highest among all the composites, was nearly 8 times higher than that of pure iron, demonstrating that an excessive addition of CS particles to iron led to accelerated degradation and this degradation rate was higher than the degradation rates of any other Fe-matrix composites studied earlier, containing relatively low amounts of bioceramics [12]. However, it should be kept in mind that the incorporation of CS into the Fe matrix could lead to a decrease in mechanical strength. Therefore, a further increase in the content of CS may not be desirable, especially when a load-bearing capacity is required for a particular orthopedic application.

From the results of the immersion tests, it is clear that the Fe-CS composites are advantageous over pure iron in terms of surface bioactivity and biodegradability. As the corrosion layer on the surfaces of the Fe-CS composites immersed in SBF is rich in Ca and P, a strengthened bonding between the implant and the surrounding bone tissue can be expected [34,35], which is highly desirable for metal-based implants. On the other hand, the faster degradation of the Fe-CS composites is preferable, as it has been proven that the inappropriately slow degradation of pure iron, despite its good biocompatibility, has made it unsuitable for application as a biodegradable implant [8]. More importantly, in this study, enhanced degradation rates of the Fe-matrix composites are achieved without alloying with elements that might raise concerns about biosafety [12,34,36]. From a biomedical point of

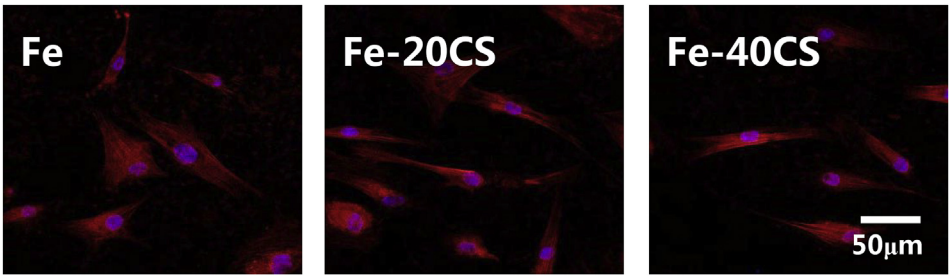

Fig. 7. F-actin staining images of HBMSCs cultured on the surfaces of Fe, Fe-20CS and Fe-40CS composites for 24 h.

view, this endows the Fe-CS composites developed in this study with additional benefits.

3.4. Cell adhesion and proliferation on the surfaces of the Fe-CS composites

Cell adhesion on pure Fe, Fe-20CS and Fe-40CS specimens was evaluated on day one by fluorescence staining for F-actin and the results are presented in Fig. 7. It can be seen that all the samples supported cell adhesion on their surfaces and the actin cytoskeletal organization was well-defined. The cells attached on the surfaces of the specimens did not show any significant differences in morphology or distribution, indicating that the incorporation of CS into iron did not exert a significant impact on cell adhesion, as compared with cell adhesion on pure Fe surface. However, it was noticed that the apparent density of cells on the surface of Fe-40CS specimen in the field of view was lower than that on iron and Fe-20CS specimens. To confirm this trend, the proliferation behavior of hBMSCs on pure Fe, Fe-20CS and Fe-40CS specimens was investigated by means of the CCK-8 assay and the results are shown in Fig. 8. It can be seen that all the specimens supported the progressive proliferation of cells with progressing time. As compared with pure iron, the Fe-20CS composite exhibited a more pronounced stimulatory effect on the proliferation of cells, whereas a further increase in CS content to 40% (Fe-40CS) showed an inhibitory effect along with prolonged incubation.

It is well known that the success of a bone implant relies on the formation of a stable and strong interface between the biomaterial and bone tissue, which involves a series of processes occurring through the initial adhesion of cells on the implant [37,38]. Therefore, cell adhesion on the surface of a bone substitution material and subsequent cellular responses, including cell proliferation, are critically important parameters for osteointegration and osteoconduction [39]. The results of the current study demonstrate that the Fe-20CS composite possesses an enhanced ability to promote the proliferation of hBMSCs, as compared with pure iron, which can be attributed to the release of Ca and Si ions from the CS component that is known for increasing cell proliferation over a certain concentration range [40,41]. Considering the fact that the osteointegration and osteoconduction behaviors of pure iron are similar to those of stainless steel [8,9], such improvements are especially desirable, when Fe-based implants are to be applied in the orthopedic field. It is however cautioned that a further increase in the content of CS to 40% will create an inhibitory effect on the proliferation of cells, as compared with pure Fe, as a result of the excessive release of Ca and Si ions from the surface of the composite or surface alkalization caused by the dissolution of the CS component [40,42]. Nevertheless, the results of this study clearly demonstrate that it is indeed feasible to improve the surface bioactivity of Fe-based materials by incorporating CS particles to the Fe matrix. Further investigations will prove the positive effect of CS on cell differentiation and in vivo bone-forming behavior.

4. Conclusions

Iron-matrix composites containing large amounts (20–40%) of calcium silicate (CS) bioceramic particles were successfully prepared by means of powder metallurgy processes. The Fe-CS composites exhibited compact structures. The bending strength of pure iron was only slightly decreased, when the content of CS was limited to 20%. Homogenously distributed CS particles in the composites induced enhanced deposition of CaP on the surfaces of specimens after immersion in the SBF solution for seven days. In addition, the degradation rates of the Fe-CS composites were significantly higher than the degradation rate of pure iron, thanks to the high solubility of the CS bioceramic in SBF. Furthermore, the composite containing 20% CS exhibited a superior ability to stimulate hBMSCs proliferation to pure iron. In summary, our study showed that calcium silicate could be an effective reinforcement phase to be added to iron or Fe-based alloys to enhance their degradation behavior and biological performance.

Acknowledgments

Financial support from the National Natural Science Foundation of China (Grant No.: 81401529 and 81671830), and the One-Hundred Talent Program of SIC-CAS (Grant No.: Y36ZB1110G) is greatly acknowledged. This work was also partly supported by the Netherlands Organisation for Health Research and Development (ZonMw) under the project 1163500004 and the Chinese Academy of Sciences (CAS) under the External Cooperation Program, Grant No. GJHZ1211.

References

[1] L. Tan, X. Yu, P. Wan, K. Yang, Biodegradable materials for bone repairs: a review, J. Mater. Sci. Technol. 29 (2013) 503–513.
[2] Z. Zhen, T. Xi, Y. Zheng, A review on in vitro corrosion performance test of biodegradable metallic materials, Trans. Nonferr. Metal. Soc. China 23 (2013) 2283–2293.
[3] C. Finkemeier, Bone-grafting and bone-graft substitutes, J. Bone Joint Surg. Am. 84 (2002) 454–464.
[4] G. Papanikolaou, K. Pantopoulos, Iron metabolism and toxicity, Toxicol. Appl. Pharmacol. 202 (2005) 199–211.
[5] B. Liu, Y. Zheng, Effects of alloying elements (Mn, Co, Al, W, Sn, B, C and S) on biodegradability and in vitro biocompatibility of pure iron, Acta Biomater. 7 (2010) 1407–1420.
[6] H. Hermawan, A. Purnama, D. Dube, J. Couet, D. Mantovani, Fe-Mn alloys for metallic biodegradable stents: degradation and cell viability studies, Acta Biomater. 6 (2010) 1852–1860.
[7] M. Peuster, C. Fink, P. Wohlsein, M. Bruegmann, A. Gunther, V. Kaese, et al., Degradation of tungsten coils implanted into the subclavian artery of New Zealand white rabbits is not associated with local or systemic toxicity, Biomaterials 24 (2003) 393–399.
[8] T. Kraus, F. Moszner, S. Fischerauer, M. Fiedler, E. Martinelli, J. Eichler, F. Witte, E. Willbold, M. Schinhammer, M. Meischel, P. Uggowitzer, J. Löffler, A. Weinberg, Biodegradable Fe-based alloys for use in osteosynthesis: outcome of an in vivo study after 52 weeks, Acta Biomater. 10 (2014) 3346–3353.
[9] M. Ulum, A. Nasution, A. Yusop, A. Arafat, M. Kadir, V. Juniantito, D. Noviana, H. Hermawan, Evidences of in vivo bioactivity of Fe-bioceramic composites for temporary bone implants, J. Biomed. Mater. Res. B Appl. Biomater. 103 (2015) 1354–1365.
[10] H. Hermawan, H. Alamdari, D. Mantovani, D. Dubé, Iron-manganese: new class of degradable metallic biomaterials prepared by powder metallurgy, Powder Metall. 51 (2008) 38–45.
[11] M. Schinhammer, A.C. Hänzi, J.F. Löffler, P.J. Uggowitzer, Design strategy for biodegradable Fe-based alloys for medical applications, Acta Biomater. 6 (2010) 1705–1713.
[12] M. Ulum, A. Arafat, D. Noviana, A. Yusop, A. Nasution, M. Abdul Kadir, H. Hermawan, In vitro and in vivo degradation evaluation of novel iron-bioceramic composites for bone implant applications, Mater. Sci. Eng. C 36 (2014) 336–344.
[13] S. Xu, K. Lin, Z. Wang, J. Chang, L. Wang, J. Lu, C. Ning, Reconstruction of calvarial defect of rabbits using porous calcium silicate bioactive ceramics, Biomaterials 29 (2008) 2588–2596.
[14] S. Ni, J. Chang, In vitro degradation, bioactivity, and cytocompatibility of calcium silicate, dimagnesium silicate, and tricalcium phosphate bioceramics, J. Biomater. Appl. 24 (2009) 139–158.
[15] X. Liu, M. Morra, A. Carpi, B. Li, Bioactive calcium silicate ceramics and coatings, Biomed. Pharmacother. 62 (2008) 526–529.
[16] J. Cheng, T. Huang, Y. Zheng, Microstructure, mechanical property, biodegradation behavior, and biocompatibility of biodegradable Fe–Fe_2O_3 composites, J. Biomed. Mater. Res. A 102 (2014) 2277–2287.
[17] K. Lin, W. Zhai, S. Ni, J. Chang, Y. Zeng, W. Qian, Study of the mechanical property and in vitro biocompatibility of $CaSiO_3$ ceramics, Ceram. Int. 31 (2005) 323–326.
[18] ASTM E9, Standard Test Methods of Compression Testing of Metallic Materials at Room Temperature, ASTM International, West Conshohocken, 2009.
[19] T. Kokubo, H. Takadama, How useful is SBF in predicting in vivo bone bioactivity? Biomaterials 27 (2006) 2907–2915.
[20] L. Yang, E. Zhang, Biocorrosion behavior of magnesium alloy in different simulated fluids for biomedical application, Mater. Sci. Eng. C 29 (2009) 1691–1696.

[21] J. Čapek, J. Kubásek, D. Vojtěch, E. Jablonská, J. Lipov, T. Ruml, Microstructural, mechanical, corrosion and cytotoxicity characterization of the hot forged FeMn30(wt.%) alloy, Mater. Sci. Eng. C 58 (2016) 900–908.
[22] T. Huang, J. Cheng, Y. Zheng, In vitro degradation and biocompatibility of Fe–Pd and Fe–Pt composites fabricated by spark plasma sintering, Mater. Sci. Eng. C 35 (2014) 43–53.
[23] H. Li, R. Daculsi, M. Grellier, R. Bareille, C. Bourget, M. Remy, et al., The role of vascular actors in two dimensional dialogue of human bone marrow stromal cell and endothelial cell for inducing self-assembled network, PLoS One 6 (2011) e16767.
[24] B. Wegener, B. Sievers, S. Utzschneider, P. Müller, V. Jansson, S. Rößler, B. Nies, G. Stephani, B. Kieback, P. Quadbeck, Microstructure, cytotoxicity and corrosion of powder-metallurgical iron alloys for biodegradable bone replacement materials, Mater. Sci. Eng. B 176 (2011) 1789–1796.
[25] S. Ni, K. Lin, J. Chang, L. Chou, β-$CaSiO_3$/β-$Ca_3(PO_4)_2$ composite materials for hard tissue repair: in vitro studies, J. Biomed. Mater. Res. A 85 (2008) 72–82.
[26] I. Ibrahim, F. Mohamed, E. Lavernia, Particulate reinforced metal matrix composites - a review, J. Mater. Sci. 26 (1991) 1137–1156.
[27] M. Nai, J. Wei, M. Gupta, Interface tailoring to enhance mechanical properties of carbon nanotube reinforced magnesium composites, Mater. Des. 60 (2014) 490–495.
[28] J. Nordin, D. Prajitno, S. Saidin, H. Nur, H. Hermawan, Structure-property relationships of iron–hydroxyapatite ceramic matrix nanocomposite fabricated using mechanosynthesis method, Mater. Sci. Eng. C 51 (2015) 294–299.
[29] E. Pagounis, V. Lindroos, Processing and properties of particulate reinforced steel matrix composites, Mater. Sci. Eng. A 246 (1998) 221–234.
[30] N. Chawla, Y. Shen, Mechanical behavior of particle reinforced metal matrix composites, Adv. Eng. Mater. 3 (2001) 357–370.
[31] C. Wu, J. Chang, A review of bioactive silicate ceramics, Biomed. Mater. 8 (2013) 032001.
[32] L.L. Hench, Bioceramics: from concept to clinic, J. Am. Ceram. Soc. 74 (1991) 1487–1510.
[33] T.S. Keller, Z. Mao, D.M. Spengler, Young's modulus, bending strength, and tissue physical properties of human compact bone, J. Orthop. Res. 8 (1990) 8592–8603.
[34] D. Yi, C. Wu, B. Ma, H. Ji, X. Zheng, J. Chang, Bioactive bredigite coating with improved bonding strength, rapid apatite mineralization and excellent cytocompatibility, J. Biomater. Appl. 28 (2014) 1343–1353.
[35] H. Mutsuzaki, Y. Sogo, A. Oyane, A. Ito, Improved bonding of partially osteomyelitic bone to titanium pins owing to biomimetic coating of apatite, Int. J. Mol. Sci. 14 (2013) 24366–24379.
[36] Q. Chen, G. Thouas, Metallic implant biomaterials, Mater. Sci. Eng. R 87 (2015) 1–57.
[37] C. Laurencin, Y. Khan, S. El-Amin, Bone graft substitutes, Expert Rev. Med. Devices 3 (2006) 49–57.
[38] V. Campana, G. Milano, E. Panago, M. Barba, C. Cicione, G. Salonna, W. Lattanzi, G. Logroscino, Bone substitutes in orthopaedic surgery: from basic science to clinical practice, J. Mater. Sci. Mater. Med. 25 (2014) 2445–2461.
[39] K. Kieswetter, Z. Schwartz, D. Dean, B. Boyan, The role of implant surface characteristics in the healing of bone, Crit. Rev. Oral. Biol. Med. 7 (1996) 329–345.
[40] P. Han, C. Wu, Y. Xiao, The effect of silicate ions on proliferation, osteogenic differentiation and cell signalling pathways (WNT and SHH) of bone marrow stromal cells, Biomater. Sci. 1 (2013) 379–392.
[41] H. Li, K. Xue, N. Kong, K. Liu, J. Chang, Silicate bioceramics enhanced vascularization and osteogenesis through stimulating interactions between endothelia cells and bone marrow stromal cells, Biomaterials 35 (2014) 3803–3818.
[42] M. Gandolfi, F. Siboni, C. Prati, Properties of a novel polysiloxane-guttapercha calcium silicate-bioglass-containing root canal sealer, Dent. Mater. 32 (2016) e113–e126.